Author(s): Belahcen, Anouar & Rasilo, Paavo & Arkkio, Antero

Title: Segregation of Iron Losses From Rotational Field Measurements and Application to Electrical Machine

Year: 2014

Version: Post print

Please cite the original version:

Belahcen, Anouar & Rasilo, Paavo & Arkkio, Antero. 2014. Segregation of Iron Losses From Rotational Field Measurements and Application to Electrical Machine. IEEE Transactions on Magnetics. Volume 50, Issue 2. 893-896. 0018-9464 (printed). DOI: 10.1109/tmag.2013.2284606.

Segregation of Iron Losses from Rotational Field Measurements and Application to Electrical Machine

A. Belahcen[1,2], P. Rasilo[1], A. Arkkio[1]

[1]Department of Electrical Engineering, Aalto University, P.O.Box 13000, FI-00076, Aalto, Finland
[2]Department of Electrical Engineering, Tallinn University of Technology, Ehitajate tee 5, Tallinn, Estonia

This paper presents a methodology for identifying a novel iron loss model and segregating the different loss components from measurements on a single sheet tester with alternating and rotating fields. The eddy current losses are first extracted with a 1D numerical approach and the hysteresis and excess losses are then estimated with an analytical method that allows the separation of alternating and rotational hysteresis as well as excess losses. The elaborated iron loss model can be applied in case of distorted flux density and on a wide range of frequencies. The identified model is further applied in the time-stepping computation of an induction motor in view of better estimation and segregation of iron losses. The results of no-load simulations at different voltage levels are in good agreement with the measured ones. All presented computations and models are validated experimentally too.

Index Terms— **Electric machines, electromagnetic analysis, loss measurement, magnetic materials, magnetic losses.**

I. Introduction

Owing to the increasing demand on high efficiency electrical motors, the designers of electrical machines need more and more accurate computation methods and estimation methodologies for the losses in these machines. The two-dimensional time-stepping finite-element method with coupled field-circuit equations is nowadays de facto standard in the design process of electrical machines. This procedure allows an accurate computation of the magnetic field in different parts of the machine as well as a rather good estimation of the resistive losses in its windings and other operation characteristics. However, this methodology is applied with a single valued BH-curve to account for the iron nonlinearity, whereas the iron losses are usually computed from different analytical equations as a posteriori quantities.

Several publications presented different methodologies for the inclusion of iron losses in the 2D FE computation of electrical machines [1]-[4]. The effect of the inclusion of iron losses in the FE computation on the operation quantities of these machines has also been investigated in [5], [6]. The main conclusion was that in machines with air gaps, i.e., rotating machines the inclusion of iron losses in the computation has very little effect on both the operation quantities and the computed iron losses, provided the loss model is accurate. It is also obvious from the literature that magnetodynamic vector hysteresis models such as the one presented in [1] and [7] can predict iron losses with higher accuracy than the analytical equations and also enables the separation of its different components. However, the identification of hysteresis models and their use in FE computations is very laborious and requires both extensive measurements for different materials before hands and prohibitive computation times during the design process. On the other hand, the analytical equations for the iron loss estimation require only few parameters but they usually do not allow for the segregation between the different loss components and their accuracy is not satisfactory.

In this paper we present a hybrid loss model in which the eddy current part is computed based on the 1D FE approach [8] and the other loss components are based on analytical equations. The identification procedure of the model is described and the predicted losses are compared with measurements on both a single sheet tester and an induction machine.

A remarkable aspect from the measurements is in the fact that the measured iron losses present a certain amount of anisotropy, which shows in the rotational losses too. Such a phenomenon needs an anisotropic model of losses.

II. Iron Loss Model

In our approach the iron power loss density in W/kg (or in same case power loss in W) is segregated into eddy-current, rotational and alternating hysteresis, and excess losses.

A. Eddy Current Losses

The Eddy current losses are computed from the magnetic flux density based on the 1D eddy current model [8], which ignores the closing path of the currents. Such a model requires only the knowledge of the magnetic flux density waveform, which in both cases of measurements and computations is well defined for both *x*- and *y*-components. The 1D eddy current problem consists of solving the diffusion system of equations

$$\begin{aligned} \frac{\partial}{\partial z}\left(\nu \frac{\partial a_x}{\partial z}\right) + \sigma \frac{\partial a_x}{\partial t} &= 0 \\ \frac{\partial}{\partial z}\left(\nu \frac{\partial a_y}{\partial z}\right) + \sigma \frac{\partial a_y}{\partial t} &= 0 \end{aligned}, \tag{1}$$

in the depth of the electrical sheet with the following boundary conditions

$$\begin{aligned} a_x(d,t) &= d.B_y(t); \quad a_x(0,t) = 0 \\ a_y(d,t) &= -d.B_x(t); \quad a_y(0,t) = 0 \end{aligned}, \tag{2}$$

where a_x and a_y are the two components of the magnetic vector potential, B_x and B_y the average flux density components, d half the thickness of the sheet and $\nu = \nu(b_x, b_y)$ the reluctivity of the magnetic material.

Manuscript received June 29, 2013. Corresponding author: Anouar Belahcen (e-mail: Anouar.belahcen@aalto.fi).
Digital Object Identifier inserted by IEEE

The 1D eddy current problem is solved numerically in a 1D finite element mesh. Note that due to the symmetry of the solution of the diffusion problem in the electrical sheet, only half of the sheet depth needs to be discretised.

B. *Hysteresis Losses*

The hysteresis losses in our model are segregated into two components, the alternating and the rotational hysteresis losses. The alternating hysteresis losses are arising from the time variation of the amplitude of the flux density vector and could be written as

$$P_{ha} = \frac{k_{ha}}{\rho T} \int_0^T |\boldsymbol{B}| \left| \frac{\partial |\boldsymbol{B}|}{\partial t} \right| dt , \qquad (3)$$

where ρ is the mass density of the material, T the time-period of one cycle of the flux density $\boldsymbol{B}$ and k_{ha} a model parameter to be estimated among other parameters. The notation $|\,|$ stands for either the absolute value of a scalar quantity or the amplitude of a vector, depending on the context.

The rotational hysteresis losses on the other hand arise from the angle between the flux density vector and its time-derivative and are expressed as

$$P_{hr} = \frac{k_{hr}}{\rho T} \int_0^T \frac{\left(1 - \frac{|\boldsymbol{B}|}{B_s}\right)}{1 + a\left(1 - \frac{|\boldsymbol{B}|}{B_s}\right)^2} \left| \frac{\boldsymbol{B}}{|\boldsymbol{B}|} \cdot \frac{\partial \boldsymbol{B}}{\partial t} \right| dt , \qquad (4)$$

where k_{hr} , a and B_s are model parameters.

C. *Excess Losses*

In Bertotti's theory of loss separation, the excess losses are compensating for the skin effect in the lamination and are also used to account for the microscopic eddy currents arising from the domains wall motion. In our model, the skin effect is accurately modeled by the 1D model but we still need to have excess losses to compensate for the domains wall motion and the interdependence between eddy current and hysteresis losses [9]. The excess losses are then mainly associated with alternating losses and they are virtually non-existing in the case of purely rotating field [10]. They are then depending only on the amplitude of the flux density and are expressed as

$$P_e = \frac{k_e}{\rho T} \int_0^T \left| \frac{\partial |\boldsymbol{B}|}{\partial t} \right|^{1.5} dt , \qquad (5)$$

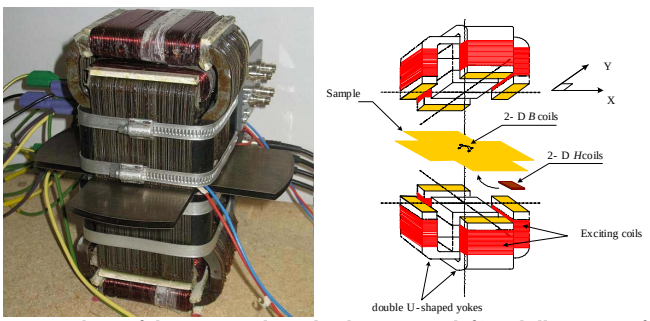

Fig. 1. Photo of the Rotational Single Sheet Tester (left) and illustration of its different parts (right). The feeding and control device are not shown.

where k_e is a model parameter. It should be noted that (3) and (5) account for alternating losses only, whereas (4) accounts for rotational losses only. In an arbitrarily varying flux density vector the losses are computed from the temporal variation of the flux density vector and integrated over one time-period.

III. Results and Discussion

The proposed model and methodology were applied locally to an electrical steel sheet with measurements results from a rotational single sheet tester (RSST) and to an induction motor at no-load. In the case of the induction machine, the no-load losses were of interest as they could be measured. Description of the applications and the related results are presented herein.

A. *Sheet Measurements and Model Prediction*

The measurements were carried out on a double-core RSST shown in Fig. 1, which allows for measurements under alternating and rotating fields [11]. The field-metric methodology was followed to compute the iron losses from the measurements. The magnetic flux density in both directions of the sheet was measured with two 2-turns search coils wound through small holes drilled in the sample. The magnetic field strength components were measured with 900-turns flat H-coils wound on top of each other and positioned parallel to the sample and in its vicinity. The alignment of the coils was secured by precision measurements and by comparing results in clockwise and anti-clockwise rotations.

The magnetizing coils of the RSST were fed from a controlled power amplifier to produce the desired magnetic flux density shape. The control was implemented in a PC-integrated fpga-acquisition card from National Instruments, with a synchronized sampling frequency of 200 kHz per channel. However, for limiting the amount of data, a down sampling methodology was used at low frequencies. A total of 250 measurements at 10 frequencies, between 10 and 1000 Hz, and varying magnetic flux densities in amplitudes and shapes have been carried out. The measured losses have been used to identify the presented iron loss model. Fig. 2 shows the measured and fitted losses. The data indices are referring to the experiment number (sorted by increasing frequencies, then by increasing amplitudes of *B*. For each frequency first x- then y-direction and last the rotational field case).

In a first, step the measured magnetic flux densities were fed to the 1D eddy current model, which computes the eddy current losses at each measurement point. The difference between the measured losses and computed eddy current losses was then used to identify the parameters of the model.

The highest peaks at low frequencies (Fig. 2 up) correspond to the measurements with rotational flux densities. It is also noted that the iron losses in rolling direction are generally smaller than the losses in transverse direction. Such anisotropy affects the accuracy of the model, which is by nature isotropic.

The breakdown of the losses into different components according to the presented model is shown in Fig. 3 for rotational 10 Hz and arbitrary 50 Hz flux densities of increasing amplitudes.

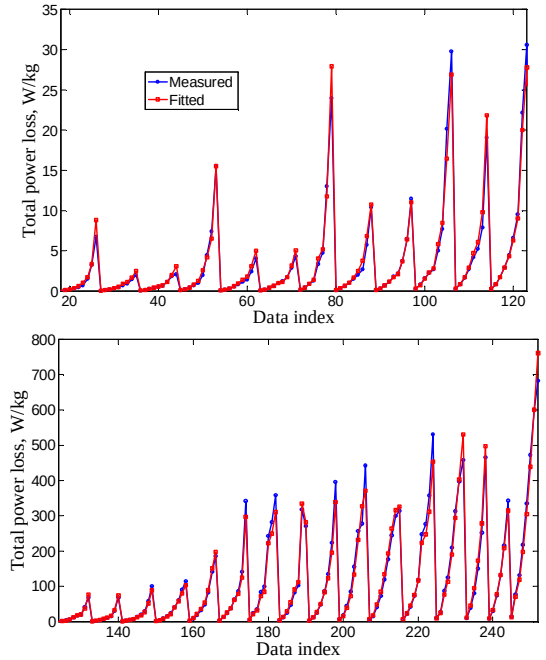

Fig. 2. Measured and model-fitted specific losses in the sample sheet at low frequencies (up) and high frequencies (down). The highest peaks at low frequencies correspond to the rotational cases. Data is sorted by frequencies then by amplitudes of flux density.

The segregated losses are qualitatively coherent with the physical understanding of the loss generation in electrical steel under alternating and rotational flux densities. Quantitatively, only the total losses can be evaluated and compared with the measurements. Here again, and regardless of slight deviations between the model and the measurement, which are partly due to the above mentioned anisotropy effects, the model seems to accurately compute the total losses.

B. *Application to Electrical Machines - Simulations*

The identified loss model has been used in the computation of iron losses in a four poles, 50 Hz, 400 V, 37 kW induction motor. The simulation of the motor was carried out with in-house 2D FE software. Second order triangular elements have been used and the iron core has been modeled with a single valued nonlinear BH-curve.

The time-stepping scheme has been applied in conjunction with the coupled field-circuit methodology to allow for voltage supply of the simulation model as well as to solve the a priori unknown rotor currents. The details of the simulation methodology and the software can be found in [12].

Within the time stepping simulations, the proposed loss model has been used to compute and segregate the different components of the losses. The 1D eddy current model has been weakly coupled to the FE 2D model of the motor and run for each integration point of the 2D triangular elements separately.

In total nine (9) no-load simulations have been carried out with increasing terminal voltages from 50 to 450 V. Plots of the rotational and alternating hysteresis loss densities in the cross section area of the motor are shown in Fig. 4. Here, one can easily see, e.g., that the rotational losses in the stator are concentrated at the bottoms and tips of the teeth, whereas they

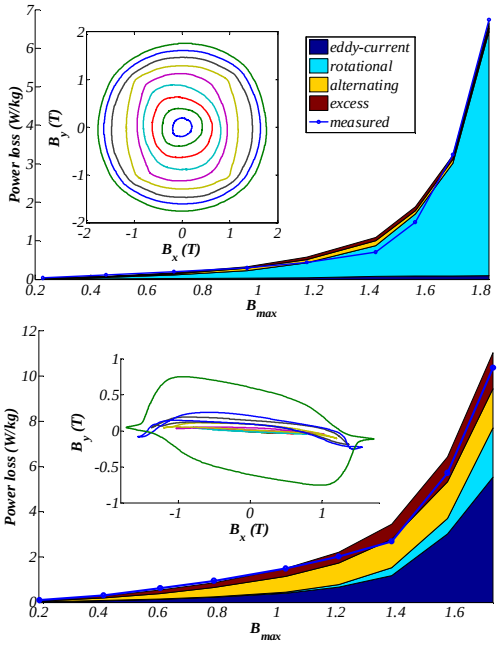

Fig. 3. Breakdown of the losses into different components according to the presented model. The upper figure shows results for 10 Hz rotational flux densities and the lower one for 50 Hz arbitrary flux densities.

are virtually zero in the middle parts of the teeth. Similarly, the alternating losses are concentrated in the middle parts of the teeth and are very low at their bottoms. In the rotor core, most of the losses are in the tips of the teeth and are generated by the higher harmonics of the magnetic flux density produced by the relative motion of the stator and rotor teeth. The losses in both stator and rotor teeth tips have contributions from both alternating and rotating ones as the magnetic flux density in these parts is very distorted in terms of harmonics and shapes.

C. *Measurements on the Electrical Machine*

On the other hand, measurements on the 37 kW induction motor have been conducted to allow for the validation of the simulations results.

The measurements on the induction machine have been carried out with the so-called slip control test [13]. In such a test, the terminals of the machine under consideration (37 kW motor) are connected to the terminals of a large-power synchronous generator through a power analyzer. The voltage at the terminals of the motor can be controlled by controlling the magnetizing current of the synchronous generator.

The shaft of the motor is coupled to the shaft of a slip-ring induction motor, the rotational speed of which is controlled by feeding its rotor at a given frequency, thus allowing the control of the slip of the motor under investigation.

Several measurements of the losses of the 37 kW motor at small values of the slip between -0.015% and 0.015% are carried out. The losses are then linearly dependent on the slip with a jump when extrapolated to zero, which is due to the hysteresis torque. The no-load losses of the motor are calculated as the average of the two extrapolated values. This method is more accurate and reliable than the standard no-load test. Other challenges related to the measurements of the no-load losses are discussed, e.g., in [13] and [14].

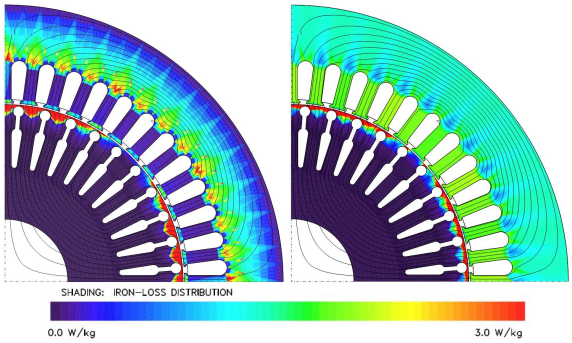

Fig. 4. Computed hysteresis loss density in the cross section of the induction machine. Left: rotational losses. Right: alternating losses. The alternating losses are absent from the stator teeth except at the teeth tips, whereas the alternating losses are almost zero at the top of the teeth.

Fig. 5 shows a comparison between the measured and computed no-load losses of the 37 kW motor. The conventional losses have been computed with the two components Steinmetz formulae applied to each harmonic.

D. Discussion

The presented methodology of iron loss computation has its roots in the loss separation theory by Bertotti [15] and the Steinmetz theory generalized by Fiorillo [16]. Our proposed model brinks a new component in these theories, namely the segregation of hysteresis loss into rotational and alternating ones, which behave in very different ways. It should be acknowledged that both theories as well as the segregation of rotational and alternating losses we presented are of phenomenological nature. However, the intensive use of these theories and models for the computation of iron losses in electrical machines over the last decades has led to a better understanding of the iron loss generation and thus to better machine designs either through optimization or expert knowledge. We believe that the use of the two hysteresis components (alternating and rotating) will increase the understanding of the loss phenomena and also contribute to the synthesis of better machine designs.

The use of the 1D eddy current model has also been used by other researchers [3], [5], [8] but its application and investigation with a rotational magnetic flux density as well as the investigation of what kind of reluctivity should be used in this case has not been reported to our knowledge.

IV. Conclusions

A phenomenological methodology to segregate the iron losses into eddy current, alternating, rotational hysteresis, and excess components has been presented. The results seem to be in good agreement with the measurements. The methodology has been applied to an induction motor and the predicted no-load losses are more accurate than the ones computed with conventional Steinmetz equations. We believe that the methodology will help in better understanding of iron loss phenomena and generating better machine designs.

Acknowledgment

The work presented in this paper has been partly supported by the funding from Tallinn University of Technology; grant B19 and SA Archimedes; MagMat project AR12131. We thank both institutions for their financial support.

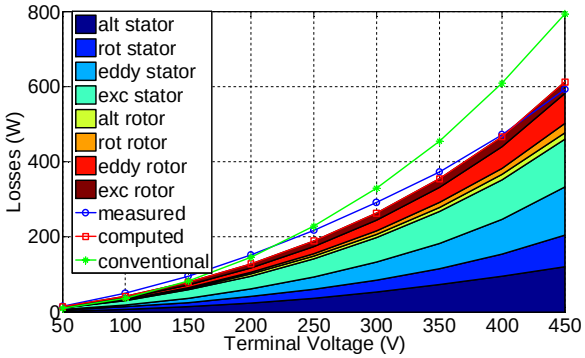

Fig. 5. Comparison of the measured and computed no-load losses in the 37 kW induction machine at different terminal voltages. The conventional losses have been computed by the Steinmetz formula applied for each harmonic separately. The area plot shows the components of the computed losses.

References

[1] E. Dlala, O. Bottauscio, M. Chiampi, M. Zucca, A. Belahcen, A. Arkkio, “Numerical investigation of the effects of loading and slot harmonics on the core losses of induction machines,” IEEE Trans. On Magn., vol. 48, no. 2, pp.1063,1066, 2012.

[2] J. Pippuri, A. Belahcen, E. Dlala, A. Arkkio, “Inclusion of eddy currents in laminations in two-dimensional finite element analysis," IEEE Trans. on Magn., vol.46, no.8, pp. 2915-2918, 2010.

[3] K. Yamazaki, N. Fukushima, “Iron loss model for rotating machines using direct eddy current analysis in electrical steel sheets,” IEEE Trans. on Energ. Conv., vol.25, no.3, pp. 633-641, 2010.

[4] N. Kunihiro, T. Todaka, M. Enokizono, “Loss evaluation of an induction motor model core by vector magnetic characteristic analysis,” IEEE Trans. on Magn., vol.47, no.5, pp. 1098-1101, 2011

[5] K. Yamazaki, N Fukushima, “Torque and loss calculation of rotating machines considering laminated cores using post 1-D analysis,” IEEE Trans. on Magn., vol.47, no.5, pp. 994-997, 2011

[6] P. Rasilo, A. Belahcen, A. Arkkio, “Importance of iron-loss modeling in simulation of wound-field synchronous machines,” IEEE Trans. on Magn., vol.48, no.9, pp. 2495-2504, 2012.

[7] E. Dlala, A. Belahcen, K.A. Fonteyn, M. Belkasim, “Improving loss properties of the Mayergoyz vector hysteresis model,” IEEE Trans. on Magn., vol.46, no.3, pp. 918-924, 2010.

[8] O. Bottauscio, M. Chiampi, D. Chiarabaglio, “Advanced model of laminated magnetic cores for two-dimensional field analysis,” IEEE Trans. on Magn., vol.36, no.3, pp. 561-573, 2000.

[9] E. Dlala, A. Belahcen, J. Pippuri, A. Arkkio, “Interdependence of hysteresis and eddy-current losses in laminated magnetic cores of electrical machines,” IEEE Trans. on Magn., vol.46, no.2, pp. 306-309, 2010.

[10] A. Cecchetti, G. Ferrari, F. Masoli and G.P. Soardo, “Rotational power losses in 3% SiFe as a function of frequency”,IEEE Trans. Magn., vol. 14, no. 5, pp. 356-358, 1978.

[11] M. Belkasim, “Identification of loss models from measurements of the magnetic properties of electrical steel sheets” M.Sc. thesis, TKK, Finland, 2008. [Online]: http://lib.tkk.fi/Dipl/2008/urn012787.pdf

[12] A. Arkkio, "Analysis of induction motors based on the numerical solution of the magnetic field and circuit equations", Ph.D. dissertation Helsinki University of Technology, 1987.

[13] J. Pippuri, and A. Arkkio, “Challenges in the segregation of losses in cage induction machines,” in Proc. of ICEM 2008, ID1445, pp.1-5.

[14] A. Boglietti, A. Cavagnino, and M. Lazzari, “Fast method for the iron loss prediction in inverter-fed induction motors”, IEEE Trans. Ind. App., vol. 46., no.2, pp. 806-811, 2010.

[15] G. Bertotti, “General properties of power losses in soft ferromagnetic materials”, IEEE Trans. Magn., vol. 24, pp. 621–630, 1988.

[16] F. Fiorillo, and A. Novikov, A., “An improved approach to power losses in magnetic laminations under nonsinusoidal induction waveform,” IEEE Trans. Magn., vol. 26, pp. 2904–2910, 1990.